Dynamic electron transport theory for multiprobe mesoscopic structures*

Quan Jun(全 军)[a], Tian Ying(田 英)[b], Zhang Jun(张 军)[a,c,†], and Shao Le-Xi(邵乐喜)[a]

[a] School of Physics Science and Technology, Zhanjiang Normal University, Zhanjiang 524048, China
[b] Center of Liberal Education, Zhanjiang Normal University, Zhanjiang 524048, China
[c] Shenzhen Institute of Advanced Integration Technology, Shenzhen 518055, China

(Received 30 December 2010; revised manuscript received 6 March 2011)

Using the linear response theory and random phase approximation, we develop a general dynamic electron transport theory for multiprobe mesoscopic structures in an arbitrarily time-dependent external field. In this case, the responses of the dynamic current, charge and internal potential to the external fields can be determined self-consistently. Without loss of generality, charge (current) conservation and gauge invariance under a potential shift are satisfied. As an example, we employ a quantum wire with a single barrier to discuss the response of the internal potential.

Keywords: mesoscopic structure, linear response theory, electron transport, quantum wire

PACS: 72.10.–d, 73.23.–b **DOI:** 10.1088/1674-1056/20/7/077201

1. Introduction

As the applications of nanostructure electronic devices increase rapidly in many fields, the electronic transport features of small conductive structures are becoming more and more important, especially for those driven by time-dependent external perturbation.[1−5] Possible future applications of nanostructures will involve high frequences, so detailed knowledge of time-dependent transport behaviour is required. The time-dependent electron transport in mesoscopic structures is strongly influenced by charging effects and the quantum effect.[1−3,6−12] The interaction and coherence of electrons also play a central role in ensuring charge (current) conservation and gauge invariance under a potential shift.[1−3,7,12] In the regime of the linear response and low-frequency approximation, Büttiker *et al.*[1−3,13] formulated the microscopic expression for the dynamic conductance of mesoscopic structures by employing continuous and discrete potential models. However, the electron–electron interaction was frequently determined by low-frequency approximation or by introducing frequency-independent geometric capacitance.[1−3,7,12] In this work, we will present a series of general and applicable formulas to self-consistently determine the dynamic charge and internal potential response to the time-dependent external fields based on the random phase approximation and linear response theory.

Before embarking on the detailed calculations, we discuss some general features of the model and the calculation. We consider a multiprobe mesoscopic structure consisting of a finite region connected to some perfectly straight semi-infinite leads, as shown in Fig. 1, and let $\boldsymbol{e}_{xm}$ be a unit vector parallel to the lead m and pointing inwards from the structure, let $\boldsymbol{e}_{ym}$ be the unit vector perpendicular to $\boldsymbol{e}_{xm}$ (defined so that one has a right-handed coordinate system $(\boldsymbol{e}_{xm}, \boldsymbol{e}_{ym}, \boldsymbol{e}_{zm})$ with $\boldsymbol{e}_{zm}$ pointing into the page), and let $S_m = |\boldsymbol{S}_m|$ be the cross-section curve of lead m. Finally, denoted by Ω, the finite screening region bounded by curve S_m. The calculation is performed self-consistently in the sense that the fields result from the voltage applied to the leads (reservoirs). Our starting points are calculating the current and charge responses to the external fields, consequently obtaining the internal potential response.

The outline of this paper is as follows: in Section 2, we will develop the general formulas for the responses of current, internal potential and charge with the aid of the linear response theory. Using the formulas obtained in Section 2, we will give some discussion and employ a quantum wire structure with a single barrier to discuss the response of the internal potential and compare it with the results given by Büttiker.

*Project supported by the Foundation for Distinguished Young Talents in Higher Education of Guangdong Province of China (Grant No. LYM10098) and the Doctor Subject Foundation of Zhanjiang Normal University of China (Grant No. ZL1004).

†Corresponding author. E-mail: rg_quan@yahoo.com.cn

© 2011 Chinese Physical Society and IOP Publishing Ltd

Some concluding remarks will be given in the last section.

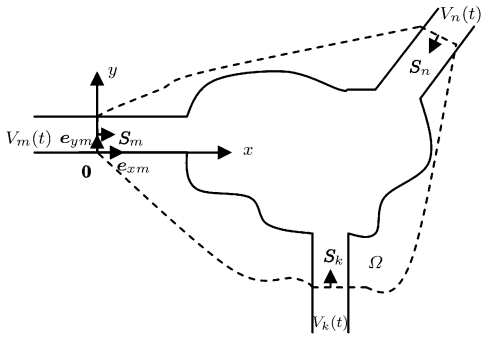


Fig. 1. Schematic view of the multiprobe mesoscopic structure in the calculation.

2. Formulation and derivation

As shown in Fig. 1, for the system in the presence of external fields, the Hamiltonian of the system is in general given by

$$H = H_0 + H'(t). \tag{1}$$

The second term $H'(t)$ in Eq. (1) represents the interaction with the external fields and accounts for the electron–electron interaction. The first term describes the unperturbed Hamiltonian in the absence of external fields and refers to the kinetic energy of electrons with momentum $\boldsymbol{p}$ at the location $\boldsymbol{r}$,

$$H_0 = \frac{\boldsymbol{p}^2}{2m_{\rm e}} + U(\boldsymbol{r}), \tag{2}$$

where $m_{\rm e}$ is the mass of the electron.

To proceed, we assume that H_0 has a complete and orthogonal set of eigenstates $\{\psi_\alpha(\boldsymbol{r})\}$ and they fulfill

$$\begin{aligned} &\int {\rm d}\boldsymbol{r}\psi^*_\alpha(\boldsymbol{r})\psi_\beta(\boldsymbol{r}) = \delta(\alpha-\beta),\\ &\int {\rm d}\alpha\psi^*_\alpha(\boldsymbol{r})\psi_\alpha(\boldsymbol{r}') = \delta(\boldsymbol{r}-\boldsymbol{r}'). \end{aligned} \tag{3}$$

Since the employed system is a finite region of arbitrary shape with an arbitrary dynamic potential connected to perfect leads (or reservoirs), the spectrum may be continuous. We therefore use an integral sign to denote both the integration over the continuous quantum number indexing the energy of the states and the summation over the discrete quantum numbers which will characterize the propagating states (channels) at fixed energy. The application of time-dependent external potential $V_m(t)$ to a reservoir m lead to the established distribution of internal potential, we have

$$H'(t) = V(\boldsymbol{r},t) = e\sum_m u_m(\boldsymbol{r},t)V_m(t), \tag{4}$$

where $u_m(\boldsymbol{r},t)$ describes the function of dynamic potential response (internal characteristic potential) to the voltage, it obeys the following requirements:[1]

1) In the depth of lead (or reservoirs) m,

$$u_m(\boldsymbol{r}_n,t) = \delta_{nm}; \tag{5}$$

2) the sum of all characteristic functions at every space point is

$$\sum_m u_m(\boldsymbol{r},t) = 1. \tag{6}$$

Let us write the perturbation in terms of its Fourier components

$$\begin{aligned} H(t') &= \int \frac{{\rm d}\omega}{2\pi}{\rm e}^{-{\rm i}\omega t}H'_\omega\\ &= e\sum_m \int \frac{{\rm d}\omega}{2\pi}{\rm e}^{-{\rm i}\omega t}u_m(\omega,\boldsymbol{r})V_m(\omega). \end{aligned} \tag{7}$$

In terms of the set of eigenstates $\{\psi_\alpha(\boldsymbol{r})\}$, the field operator $\hat{\Psi}(\boldsymbol{r})$ and its conjugation are a linear combination of the states $\psi_\alpha(\boldsymbol{r})$ in the so-called second quantized form

$$\begin{aligned} \hat{\Psi}(\boldsymbol{r}) &= \int {\rm d}\alpha\hat{a}_\alpha\psi_\alpha(\boldsymbol{r}),\\ \hat{\Psi}^\dagger(\boldsymbol{r}) &= \int {\rm d}\alpha\hat{a}^\dagger_\alpha\psi^*_\alpha(\boldsymbol{r}), \end{aligned} \tag{8}$$

where $\hat{a}_\alpha(\hat{a}^\dagger_\alpha)$ is the annihilation (creation) operator for a particle at energy ε_α, with this we obtain the frequency-dependent H'_ω in the form of second quantization,

$$H'_\omega = e\sum_m \int {\rm d}\alpha \int {\rm d}\beta u^m_{\alpha\beta}(\omega)\delta V_m(\omega)\hat{a}^\dagger_\alpha\hat{a}_\beta, \tag{9}$$

with

$$u^m_{\alpha\beta}(\omega) = \int \psi^*_\alpha(\boldsymbol{r})u_m(\omega,\boldsymbol{r})\psi_\beta(\boldsymbol{r})\,{\rm d}\boldsymbol{r}. \tag{10}$$

The current density operator is

$$\hat{\boldsymbol{J}}(\boldsymbol{r}) = e\int {\rm d}\alpha \int {\rm d}\beta \boldsymbol{J}_{\alpha\beta}(\boldsymbol{r})\hat{a}^\dagger_\alpha\hat{a}_\beta, \tag{11}$$

with

$$\boldsymbol{J}_{\alpha\beta}(\boldsymbol{r}) = \frac{{\rm i}\hbar}{2m_{\rm e}}\psi^*_\alpha(\boldsymbol{r})\overleftrightarrow{\boldsymbol{\nabla}}\psi_\beta(\boldsymbol{r}),$$

where we simplify the notation by introducing the double-sided derivative operator defined with respect to the two arbitrary functions, F and G, by

$$F\overleftrightarrow{\boldsymbol{\nabla}}G = F\boldsymbol{\nabla}G - G\boldsymbol{\nabla}F. \tag{12}$$

Hence, the current operator through the cross section of the mth lead is

$$\begin{aligned}\hat{I}_m(\boldsymbol{r}_m) &= \int_{S_m} \hat{J}(\boldsymbol{r}_m)\cdot \mathrm{d}\boldsymbol{S}_m \\ &= e\int \mathrm{d}\alpha \int \mathrm{d}\beta \int_{S_m} \boldsymbol{J}_{\alpha\beta}(\boldsymbol{r}_m)\cdot \mathrm{d}\boldsymbol{S}_m \hat{a}^{\dagger}_{\alpha}\hat{a}_{\beta} \\ &= e\int \mathrm{d}\alpha \int \mathrm{d}\beta I_{\alpha\beta}(x_m)\hat{a}^{\dagger}_{\alpha}\hat{a}_{\beta}. \end{aligned} \tag{13}$$

According to the general linear response theory, the expectation value of current responses to voltage is

$$\begin{aligned}&\delta I_m(\omega) \\ &= -\frac{\mathrm{i}}{\hbar}\int_{-\infty}^{+\infty} \mathrm{d}\tau\theta(\tau)\mathrm{e}^{\mathrm{i}(\omega+\mathrm{i}\eta^{\dagger})\tau}\langle[\hat{I}^I_m(x_m,\tau), H'^I_{\omega}]\rangle_0. \end{aligned} \tag{14}$$

Note that the infinitesimal $\eta^{\dagger}$ is incorporated in order to ensure the correct physical result, and $\langle[\,]\rangle_0$ denotes thermodynamic average for the systems described by H_0, $\hat{I}^I_m(x_m,\tau) = \mathrm{e}^{-H_0 t/\hbar}\hat{I}_m(x_m,\tau)\mathrm{e}^{H_0 t/\hbar}$. Inserting Eqs. (9) and (13) into Eq. (14), we arrive at the main result of this part of the calculation

$$\begin{aligned}\delta I_m(\omega) &= -e^2\sum_n \int \mathrm{d}\alpha \int \mathrm{d}\beta I_{\alpha\beta}(x_m)u^n_{\beta\alpha}(\omega) \\ &\quad\times \frac{n_\alpha - n_\beta}{\varepsilon_\alpha - \varepsilon_\beta + \hbar\omega + \mathrm{i}\hbar\eta^{\dagger}}\delta V_n(\omega), \end{aligned} \tag{15}$$

where $n_\alpha(n_\beta)$ refers to the Fermi–Dirac distribution function. Linearizing Eq. (15), we obtain

$$\delta I_m = \sum_n G_{mn}(\omega)\delta V_n(\omega), \tag{16}$$

where $G_{mn}(\omega)$ are the conductance coefficients in the frequency domain and are given by

$$\begin{aligned}G_{mn}(\omega) &= -e^2\int \mathrm{d}\alpha \int \mathrm{d}\beta I_{\alpha\beta}(x_m)u^n_{\beta\alpha}(\omega) \\ &\quad\times \frac{n_\alpha - n_\beta}{\varepsilon_\alpha - \varepsilon_\beta + \hbar\omega + \mathrm{i}\hbar\eta^{\dagger}}. \end{aligned} \tag{17}$$

Using the identity in Eq. (11), we obtain

$$\psi^*_\alpha(\boldsymbol{r})\psi_\beta(\boldsymbol{r}) = \frac{\hbar}{\mathrm{i}(\varepsilon_\beta - \varepsilon_\alpha)}\boldsymbol{\nabla}\cdot\boldsymbol{J}_{\alpha\beta}(\boldsymbol{r}). \tag{18}$$

Taking into account the boundary conditions in Eqs. (5) and (6), we obtain

$$\begin{aligned}u^m_{\beta\alpha}(\omega) &= \int_{\bar{\Omega}} \psi^*_\beta(\boldsymbol{r})\psi_\alpha(\boldsymbol{r})\mathrm{d}\boldsymbol{r} \\ &\quad+ \int_{\Omega} \psi^*_\beta(\boldsymbol{r})u_n(\omega,\boldsymbol{r})\psi_\alpha(\boldsymbol{r})\mathrm{d}\boldsymbol{r}. \end{aligned} \tag{19}$$

Substituting Eq. (18) into Eq. (19), we have

$$\begin{aligned}u^m_{\beta\alpha}(\omega) &= \frac{\hbar}{\mathrm{i}(\varepsilon_\alpha - \varepsilon_\beta)}\int_{\Omega_m} \boldsymbol{\nabla}\cdot\boldsymbol{J}_{\beta\alpha}(\boldsymbol{r})\mathrm{d}\boldsymbol{r} \\ &\quad+ \int_{\Omega} \psi^*_\beta(\boldsymbol{r})u_n(\omega,\boldsymbol{r})\psi_\alpha(\boldsymbol{r})\mathrm{d}\boldsymbol{r}, \end{aligned} \tag{20}$$

where Ω_m denotes the region of reservoir m.

Integrating Eq. (20) and using the divergence theorem, we obtain

$$\begin{aligned}u^m_{\beta\alpha}(\omega) &= \frac{\hbar}{\mathrm{i}(\varepsilon_\alpha - \varepsilon_\beta)}I_{\beta\alpha}(x_m) \\ &\quad+ \int_{\Omega} \psi^*_\beta(\boldsymbol{r})u_n(\omega,\boldsymbol{r})\psi_\alpha(\boldsymbol{r})\mathrm{d}\boldsymbol{r}. \end{aligned} \tag{21}$$

Hence, $G_{mn}(\omega)$ in Eq. (17) can be cast into

$$G_{mn}(\omega) = G^{\mathrm{ext}}_{mn}(\omega) + \int_{\Omega} g_m(\boldsymbol{r})u_n(\omega,\boldsymbol{r})\mathrm{d}\boldsymbol{r}, \tag{22}$$

where

$$\begin{aligned}G^{\mathrm{ext}}_{mn}(\omega) &= \mathrm{i}\hbar e^2\int \mathrm{d}\alpha \int \mathrm{d}\beta \frac{I_{\alpha\beta}(x_m)I_{\beta\alpha}(x_n)}{\varepsilon_\beta - \varepsilon_\alpha} \\ &\quad\times \frac{n_\alpha - n_\beta}{\varepsilon_\alpha - \varepsilon_\beta + \hbar\omega + \mathrm{i}\hbar\eta^{\dagger}}, \end{aligned} \tag{23}$$

$$\begin{aligned}g_m(\boldsymbol{r}) &= -e^2\int \mathrm{d}\alpha \int \mathrm{d}\beta I_{\alpha\beta}(x_m)\int_{\Omega} \psi^*_\beta(\boldsymbol{r})\psi_\alpha(\boldsymbol{r})\mathrm{d}\boldsymbol{r} \\ &\quad\times \frac{n_\alpha - n_\beta}{\varepsilon_\alpha - \varepsilon_\beta + \hbar\omega + \mathrm{i}\hbar\eta^{\dagger}}. \end{aligned} \tag{24}$$

The operator of the electrical charge density $\hat{\rho}(\boldsymbol{r})$ is defined as

$$\hat{\rho}(\boldsymbol{r}) = -e\hat{\Psi}^{\dagger}(\boldsymbol{r})\hat{\Psi}(\boldsymbol{r}). \tag{25}$$

In terms of the operators $\hat{a}^{\dagger}_\alpha$ and $\hat{a}_\beta$, $\hat{\rho}(\boldsymbol{r})$ can be written as

$$\hat{\rho}(\boldsymbol{r}) = -e\int \mathrm{d}\alpha \int \mathrm{d}\beta \psi^*_\alpha(\boldsymbol{r})\psi_\beta(\boldsymbol{r})\hat{a}^{\dagger}_\alpha\hat{a}_\beta. \tag{26}$$

Using a similar procedure to the deviation of conductance coefficients, we can write the expression for the response of charge density

$$\begin{aligned}&\delta\rho_m(\boldsymbol{r},\omega) \\ &= \rho^{\mathrm{ext}}_m(\boldsymbol{r},\omega) + \int_{\Omega} \Pi(\boldsymbol{r},\boldsymbol{r}')u_m(\omega,\boldsymbol{r}')\mathrm{d}\boldsymbol{r}', \end{aligned} \tag{27}$$

where

$$\begin{aligned}\rho^{\mathrm{ext}}_m(\boldsymbol{r},\omega) &= \mathrm{i}\hbar e^2\int \mathrm{d}\alpha \int \mathrm{d}\beta \frac{I_{\alpha\beta}(x_m)\psi^*_\beta(\boldsymbol{r})\psi_\alpha(\boldsymbol{r})}{\varepsilon_\beta - \varepsilon_\alpha} \\ &\quad\times \frac{n_\alpha - n_\beta}{\varepsilon_\alpha - \varepsilon_\beta + \hbar\omega + \mathrm{i}\hbar\eta^{\dagger}}, \end{aligned} \tag{28}$$

$$\begin{aligned}\Pi(\boldsymbol{r},\boldsymbol{r}',\omega) &= e^2\int \mathrm{d}\alpha \int \mathrm{d}\beta\psi^*_\alpha(\boldsymbol{r})\psi_\beta(\boldsymbol{r})\psi^*_\beta(\boldsymbol{r}')\psi_\alpha(\boldsymbol{r}') \\ &\quad\times \frac{n_\alpha - n_\beta}{\varepsilon_\alpha - \varepsilon_\beta + \hbar\omega + \mathrm{i}\hbar\eta^{\dagger}}. \end{aligned} \tag{29}$$

Finally, the internal characteristic potential can be obtained via the Poisson equation

$$\boldsymbol{\nabla}^2 u_m(\omega,\boldsymbol{r}) + \frac{1}{\varepsilon_0}\int \Pi(\boldsymbol{r},\boldsymbol{r}',\omega)\,\mathrm{d}\boldsymbol{r}' = -\frac{1}{\varepsilon_0}\rho_m^{\mathrm{ext}}(\boldsymbol{r},\omega). \tag{30}$$

To make further progress, take the limit as $\eta^\dagger$ goes to zero and using

$$\lim_{\eta^\dagger\to 0}\frac{1}{x\pm \mathrm{i}\eta^\dagger} = -\mathrm{i}\pi\delta(x) + \mathrm{P}\left[\frac{1}{x}\right], \tag{31}$$

where P indicates a principal-value integral, we have

$$\mathrm{Re}\,[G_{mn}^{\mathrm{ext}}(\omega)] = \pi\hbar e^2\int \mathrm{d}\alpha I_{\alpha\beta}(x_m)I_{\beta\alpha}(x_m) \times \frac{n_\alpha(\varepsilon_\alpha) - n_\alpha(\varepsilon_\alpha+\hbar\omega)}{\hbar\omega}. \tag{32}$$

Similarly,

$$\mathrm{Im}\,[g_m(\boldsymbol{r})] = \pi e^2\int \mathrm{d}\alpha\int I_{\alpha\beta}(x_m)\int_\Omega \psi_\beta^*(\boldsymbol{r})\psi_\alpha(\boldsymbol{r})\,\mathrm{d}\boldsymbol{r} \times [n_\alpha(\varepsilon_\alpha) - n_\alpha(\varepsilon_\alpha+\hbar\omega)], \tag{33}$$

$$\mathrm{Re}\,[\rho_m^{\mathrm{ext}}(\boldsymbol{r},\omega)] = \pi\hbar e^2\int \mathrm{d}\alpha I_{\alpha\beta}(x_m)\psi_\beta^*(\boldsymbol{r})\psi_\alpha(\boldsymbol{r}) \times \frac{n_\alpha(\varepsilon_\alpha) - n_\alpha(\varepsilon_\alpha+\hbar\omega)}{\hbar\omega}, \tag{34}$$

$$\mathrm{Im}\,[\Pi(\boldsymbol{r},\boldsymbol{r}',\omega)] = e^2\int \mathrm{d}\alpha\psi_\alpha^*(\boldsymbol{r})\psi_\beta(\boldsymbol{r})\psi_\beta^*(\boldsymbol{r}')\psi_\alpha(\boldsymbol{r}') \times [n_\alpha(\varepsilon_\alpha) - n_\alpha(\varepsilon_\alpha+\hbar\omega)]. \tag{35}$$

The real (imaginary) parts of these quantities then can be obtained by applying the Kramers–Kronig relation, for example,

$$\mathrm{Im}\,[G_{mn}^{\mathrm{ext}}(\omega)] = \frac{2}{\pi}\mathrm{P}\int \frac{v\mathrm{Re}\,[G_{mn}^{\mathrm{ext}}(\omega)]}{v^2-\omega^2}\,\mathrm{d}v. \tag{36}$$

We have now arrived at our main results, which determine the $G_{mn}^{\mathrm{ext}}(\omega)$, $\rho_m^{\mathrm{ext}}(\omega,\boldsymbol{r})$ and $u_m(\omega,\boldsymbol{r})$ self-consistently.

3. Discussion and example

3.1. External conductance and interacting conductance

The first term on the right-hand side of Eq. (22) corresponds to the external (or non-interacting) conductance $G_{mn}^{\mathrm{ext}}(\omega)$ in the scattering theory given by Büttiker. In the scattering theory, the $G_{mn}^{\mathrm{ext}}(\omega)$ is given by

$$G_{mn}^{\mathrm{ext}}(\omega) = \frac{e^2}{\hbar}\int \mathrm{d}E\mathrm{Tr}\,[\hat{1}_\alpha(E)\delta_{\alpha\beta} - s_{\alpha\beta}^\dagger(E)s_{\alpha\beta}(E+\hbar\omega)] \times \frac{n_\beta(E) - n_\alpha(E)}{\hbar\omega}. \tag{37}$$

In the low frequency case, we obtain a similar expression if we take the scattering-state wave as the eigenfunctions in the leads. However, for high frequency there are some differences between them. The second term corresponds to the interacting conductance, which is given by $G_{mn}^{\mathrm{int}}(\omega) = \int g_m(\boldsymbol{r},\omega)u_n(\boldsymbol{r},\omega)\mathrm{d}\boldsymbol{r}$. From this expression, it indicates that the AC conductance depends on the spatial shape of the internal potential. In a general DC case, this term should vanish. It can be proved easily by using the identity in Eqs. (3) and (18).

3.2. Current conservation

Using the charge conservation equation $\boldsymbol{\nabla}\cdot\boldsymbol{J} = \mathrm{i}\omega\rho$, one can easily obtain the charge conservation by applying the linear response theory to the current-density operator of Eq. (11) and using Eqs. (18) and (28). Moreover, if the area Ω is large enough, and in each lead the solution of the Poisson equation fulfills $\boldsymbol{\nabla}u_m(\omega,\boldsymbol{r}) = 0$, then it is easy to prove $\sum_m \delta I_m = 0$, namely $\sum_m G_{mn}(\omega) = 0$. Therefore, the AC conductance will naturally satisfy current conservation. Moreover, in our calculation all the responses are obtained within the framework of linear response theory, and the conservation of charge and current is satisfied naturally.

3.3. An example: a quantum wire structure with a single barrier

As an application of the theory, we employ a typical mesoscopic example, i.e. a quantum wire with a single barrier connected to two wide reservoirs, as depicted in Fig. 2. Here, we assume that the whole structure and parts of the reservoirs are in the screening area Ω (the dashed line box in Fig. 2), which is very large and includes all the varying distributions of the potential and charges. This means that all the electric-field lines come from and end at the charges inside the volume. When an AC bias potential with frequency ω is applied at reservoir α, we should consider the scattering of electrons at the contact. Hence, the scattering state wave function with wave vector $\boldsymbol{k}$ and energy E incident on the channel opening from the left can be written as

$$\psi_l^{\mathrm{L}}(x,y) = \sum_{l'}\left(\delta_{ll'}\,\mathrm{e}^{\mathrm{i}k_l^x x} + r_{11,ll'}\mathrm{e}^{-\mathrm{i}k_{l'}^x x}\right)\varphi_{l'}^{\mathrm{2D}}(y). \tag{38}$$

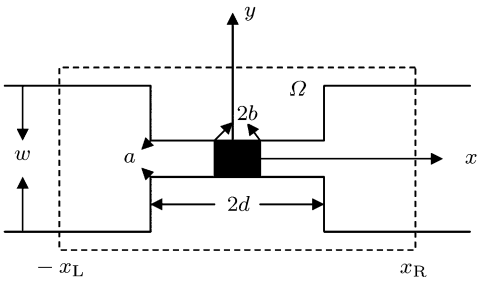


Fig. 2. Schematic view of a quantum wire with a single barrier connected to two wide reservoirs (Ω is a screening area and no electrical field line penetrates its surface).

For the electron in $x > d$, the wave function can be written as

$$\psi_l^{\mathrm{R}}(x,y) = \sum_{l'} t_{21,ll'} \mathrm{e}^{\mathrm{i}k_{l'}^x x} \varphi_{l'}^{\mathrm{2D}}(y), \tag{39}$$

where $\varphi_{l'}^{\mathrm{2D}}(y)$ is the transverse wave function for mode l, $k_{l'}^x$ can be either real or imaginary, namely, evanescent waves are included and given by $k_{l'}^x = [2m_eE/\hbar^2 - (l'\pi/w)^2]^{1/2}$, $l \in [0, \mathrm{int}[(2m_ewE/\pi^2\hbar^2)^{1/2}]]$. Here, we introduce scattering matrix elements $s_{11,ll'}$ and $s_{21,ll'}$,

$$r_{11,ll'} = \left(\frac{v_l}{v_{l'}}\right)^{1/2} s_{11,ll'}, \quad t_{21,ll'} = \left(\frac{v_l}{v_{l'}}\right)^{1/2} s_{21,ll'},$$
$$v_l = \frac{\hbar k_l^x}{m_e}. \tag{40}$$

The sum in Eqs. (38) and (39) is taken over all transverse components.

The one-dimensional (1D) structure including a single barrier together with the left and right leads is divided into three portions. The wave function may be expanded as

$$\psi_l^{\mathrm{c}}(x,y) = \sum_n \left[A_{nl}^{(I)} \mathrm{e}^{\mathrm{i}k_n^{(I)}x} + B_{nl}^{(I)} \mathrm{e}^{-\mathrm{i}k_n^{(I)}x}\right] \Phi_n^{\mathrm{1D}}(y), \tag{41}$$

where, $I = 1, 2, 3$ denote various regions of the 1D structure, $\Phi_n^{\mathrm{1D}}(y)$ are the transverse eigenfunctions of electrons in this region, $k_n^{x(I)} = [2m_{\mathrm{e}}(E - U_I)/\hbar^2 - (n\pi/a)^2]^{1/2}$, U_I is the single-barrier potential and is given by

$$U_I = \begin{cases} U_0, & \text{in the barrier,} \\ 0, & \text{else.} \end{cases} \tag{42}$$

Similarly, the scattering wave functions incident from the right lead are

$$\psi_l(x,y)|_{\mathrm{R}} = \psi_l(-x,y)|_{\mathrm{L}}. \tag{43}$$

At the boundaries of the various regions, we match the wave function and their derivatives, and this gives the desired transmission coefficients

$$\sum_n \left[A_{nl}^{(I)} \mathrm{e}^{\mathrm{i}k_n^{(I)}x_I} + B_{nl}^{(I)} \mathrm{e}^{-\mathrm{i}k_n^{(I)}x_I}\right] \Phi_n^{\mathrm{1D}}(y)$$
$$= \sum_n \left[A_{nl}^{(I)} \mathrm{e}^{\mathrm{i}k_n^{(I+1)}x_I} + B_{nl}^{(I+1)} \mathrm{e}^{-\mathrm{i}k_n^{(I+1)}x_I}\right] \Phi_n^{\mathrm{1D}}(y), \tag{44}$$

$$\sum_n k_n^{x(I)} \left[A_{nl}^{(I)} \mathrm{e}^{\mathrm{i}k_n^{(I)}x_I} - B_{nl}^{(I)} \mathrm{e}^{-\mathrm{i}k_n^{(I)}x_I}\right] \Phi_n^{\mathrm{1D}}(y)$$
$$= \sum_n k_n^{x(I+1)} \left[A_{nl}^{(I+1)} \mathrm{e}^{\mathrm{i}k_n^{(I+1)}x_I} - B_{nl}^{(I+1)} \mathrm{e}^{-\mathrm{i}k_n^{(I+1)}x_I}\right] \times \Phi_n^{\mathrm{1D}}(y), \tag{45}$$

where x_I is the interface position between regions I and $I+1$. Thus, the transfer relationship can be obtained as

$$\begin{bmatrix} A^{(I)}(x) \\ B^{(I)}(x) \end{bmatrix} = \prod_{J=1}^{3} M_J \begin{bmatrix} A^{(J)}(x) \\ B^{(J)}(x) \end{bmatrix}, \tag{46}$$

where M_J is the transfer matrix element between regions J and $J+1$.

The continuity of $\psi_l^{\mathrm{L}}(x,y), \psi_l^{\mathrm{R}}(x,y)$ and $\psi_l^{\mathrm{c}}(x,y)$ at $x = \pm d$ yields

$$\sum_n \left[\left(T_{mn} - k_n^{x(1)}\delta_{mn}\right) A_{nl}^{(1)} \mathrm{e}^{\mathrm{i}k_n^{x(1)}d} + \left(\left(T_{mn} - k_n^{x(1)}\delta_{mn}\right) B_{nl}^{(1)} \mathrm{e}^{\mathrm{i}k_n^{x(1)}d}\right)\right]$$
$$= 2k_l^x M_{lm} \mathrm{e}^{-\mathrm{i}k_l^x d}, \tag{47}$$

$$\sum_n \left[(T_{mn} - k_n^{x(3)}\delta_{mn}) A_{nl}^{(3)} \mathrm{e}^{\mathrm{i}k_n^{x(5)}d} + (T_{mn} + k_n^{x(3)}\delta_{mn}) B_{nl}^{(3)} \mathrm{e}^{\mathrm{i}k_n^{x(3)}d}\right]$$
$$= 0, \tag{48}$$

where

$$M_{lm} = \int \left(\varphi_l^{\mathrm{2D}}(y)\right)^* \Phi_m^{\mathrm{1D}}(y) \mathrm{d}y,$$
$$T_{mn} = \sum_l k_l^x M_{lm}^* M_{ln}. \tag{49}$$

Hence, the scattering matrix elements $s_{11,ll'}$ and $s_{21,ll'}$ can be calculated by the following equations:

$$s_{11,ll'} = -\delta_{ll'} \left(\frac{v_{l'}}{v_l}\right)^{1/2} \mathrm{e}^{-\mathrm{i}(k_{l'}^x + k_l^x)d} + \sum_n \left(\frac{v_{l'}}{v_l}\right)^{1/2} M_{l'n} \Big(A_{nl}^{(1)} \mathrm{e}^{-\mathrm{i}\left(k_{l'}^{(1)x} + k_l^x\right)d} + B_{nl}^{(1)} \mathrm{e}^{\mathrm{i}(k_{l'}^{(1)x} - k_l^x)d}\Big),$$

$$s_{21,ll'} = \sum_n \left(\frac{v_{l'}}{v_l}\right)^{1/2} M_{l'n} \Big(A_{nl}^{(3)} \mathrm{e}^{-\mathrm{i}\left(k_{l'}^{(3)x} + k_l^x\right)d}$$

$$+ B_{nl}^{(3)} \mathrm{e}^{\mathrm{i}\left(k_{l'}^{(3)x} - k_l^x\right)d}\Big). \tag{50}$$

In order to verify our theory, we discuss below the distribution of internal response potential for different cases. For convenience of calculation, we take the width of the leads ($a = 50$ nm) and the transverse ground-state energy $\Delta = \pi^2\hbar^2/2m_{\mathrm{e}}a^2$ in the 1D leads as the units of length and energy, respectively. $x_{\mathrm{L}} = x_{\mathrm{R}}$. In the following discussion we can express an integral over these scattering states explicitly in terms of an integral over energy, that is to say, $\int \mathrm{d}\alpha \to \sum_{\alpha m} \int (\mathrm{d}E_{\alpha m}/\sqrt{h}v_{\alpha m})$. Hence, we can obtain the distribution of internal potential in terms of the scattering wave function and Eqs. (30), (34)–(36).

In Fig. 3(a) we present the distribution of the internal characteristic potential for different cases at temperature $T = 0, w = 50, b = 0.5$. For the case without a barrier (where $U_0 = 0, E_{\mathrm{F}} = 1.6$), one finds $u(x) = 1(0)$ in the left (right) lead, but it decreases gradually when it penetrates the left contact, and remains unchanged in the 1D portion ($u(x) = 1/2$), and the potential drop appears in the transition region between the 1D and 2D portions. For $U_0 = 3$, it corresponds to the case of small transmission probability, the result shows that the potential drop happens mainly within the barrier and $u(x) = 1(0)$ beyond the barrier. In this case, the charges driven to the other side of the conductor penetrate through the barrier with a small transmission probability. Thus, most of the charge carriers are reflected back into the 1D leads and reservoir. Therefore, there is no charge accumulation beyond the barrier, and the internal potential $u(x)$ should be constant (1) beyond the barrier. Furthermore, with the increase of the Fermi energy, the potential drop between the barrier and reservoirs will increase. It is worth noting that not only does the potential drop appear in the contacts, but also in the leads, and there are some oscillations in the potential in the 1D leads. This fulfills the requirement of Büttiker's theory.

For a given Fermi energy (Here, $U_0 = 3, E_{\mathrm{F}} = 2.4$), we find that the internal characteristic potential depends on the frequency of the external fields, as shown in Fig. 3(b). Results show that the potential drop will increase with the increase of the frequency, especially in the region of the contacts.

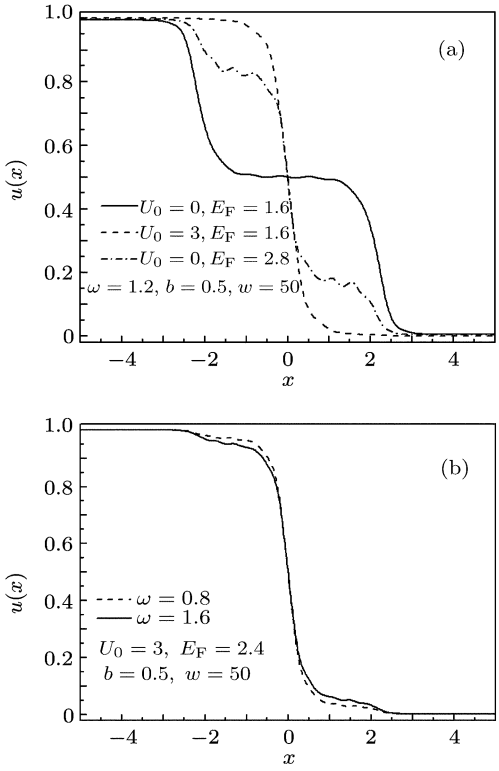


Fig. 3. The distribution of the internal characteristic potential (a) in different cases and (b) for different frequencies.

From the results given in Figs. 3(a) and 3(b), we find that the internal characteristic potential is continuous at the boundaries, and even anywhere in screening area. It is not surprising that the internal characteristic potential is the response of the internal potential to the external voltage or fields. In the example given by us, we assume that the whole single barrier structure and parts of reservoirs are in the screening area, which is very large and includes all the various distributions of the potential and charges. As mentioned above, all the electric-field lines come from and end at the charges inside the volume, but not screening the internal potential,[1] so the internal potential is continuous, namely the internal characteristic potential is also continuous.

4. Conclusion

In conclusion, we have provided an approach to calculating the dynamic responses of a multiprobe mesoscopic structure to external fields within the framework of linear response theory, and explicitly presented the general formulation for calculating the external conductance, local-current response and external charge density. This allows us to self-consistently obtain the dynamic conductance, internal characteristic potential and charge distribution

induced by the external fields. Furthermore, we illustrated that our formulae for this theory naturally satisfy the charge and current conservation, as well as gauge invariance conditions under a potential shift. As an application, we also discussed the internal characteristic potential of a quantum wire structure, and our results are in conformity with Büttiker's conclusion for a given frequency, especially at low frequency.

References

[1] Büttiker M 1993 *J. Phys. Condens. Matter* **5** 9361

[2] Christen T and Büttiker M 1996 *Phys. Rev. Lett.* **77** 143

[3] Büttiker M, Pretre A and Thomas H 1993 *Phys. Rev. Lett.* **70** 4114

[4] Li X Q, Luo J Y, Yang Y G, Cui P and Yan Y J 2005 *Phys. Rev.* B **71** 205304

[5] Li X Q and Su Z B 1996 *Phys. Rev.* B **54** 10807

[6] Ji Y H, Lei M S and Ouyang C Y 2002 *Chin. Phys.* **11** 163

[7] Büttiker M and Martin A M 2000 *Phys. Rev.* B **61** 2737

[8] Dong Z C 1999 *Acta Phys. Sin.* **48** 511 (in Chinese)

[9] Li T C and Lu P S 2008 *Phys. Rev.* B **77** 85408

[10] Xu H and Song W P 2002 *Acta Phys. Sin.* **51** 1798 (in Chinese)

[11] Wang C and Zhang Y H 2006 *Chin. Phys.* **15** 2120

[12] Wang J, Guo H, Jose-Luis M, Wan C C, Taraschi G and Zheng Q R 1998 *Phys. Rev. Lett.* **80** 4277

[13] Pretre A, Thomas H and Büttiker M 1996 *Phys. Rev.* B **54** 8130